Nanoscale

RSC Publishing

PAPER

View Article Online
View Journal | View Issue

# Self-stopping effects of lithium penetration into silicon nanowires

Cite this: *Nanoscale*, 2013, **5**, 12394

Li Lang,[a] Chuanding Dong,[a] Guohong Chen,[a] Jihui Yang,[a] Xiao Gu,[a] Hongjun Xiang,[a] Ruqian Wu[b] and Xingao Gong[a]

Received 27th June 2013
Accepted 13th September 2013

DOI: 10.1039/c3nr03301e

www.rsc.org/nanoscale

Using first-principles molecular dynamics simulations, we demonstrate that the penetration of lithium atoms into a silicon nanowire (SiNW) self-stops once a metallic amorphous Li–Si shell forms. This explains the extended life of crystalline Si cores in SiNW battery electrodes observed in experiments. Metallic Li–Si shells grasp Li atoms and prohibit them from directly segregating through interstitial channels toward the crystalline center of SiNWs. Meanwhile, high pressure develops on the core as it shrinks, due to the expansion and tension in the amorphous shell, which eventually frustrate the step-forward amorphization. We also elucidate the reasons why H-passivated SiNWs are not suitable for studies of lithiation processes.

Published on 17 September 2013. Downloaded by Fudan University on 24/03/2014 03:37:17.

## Introduction

Silicon nanowires (SiNWs) have been widely used as prototype nanostructures in the last decade as they are ideal building blocks for various miniaturized devices such as nanosensors,[1] nanoelectronics[2,3] and energy storage devices.[4,5] One particularly promising application of SiNWs is to use them as anode materials in high performance Li-ion batteries.[6] Compared with conventional graphite anodes, silicon has much higher charge capacity (4200 mA h $g^{-1}$),[6] lower discharge potential and lower cost. However, the development of silicon anode materials in Li-ion batteries is nontrivial due to the exceedingly large volume changes (~300%) during lithium insertion and extraction.[7] The Li–Si intermixing mechanism during lithiation and the lithiation-induced volume expansion in silicon have been widely investigated. In particular, the anisotropic Li distribution in Si as well as the orientation dependent penetration of Li into different Si surfaces has been revealed in ref. 8–13. To prevent Si from Li-induced pulverization, Si-based nanostructures such as nanoparticles,[14,15] nanowires,[6,16–18] and nanotubes[19,20] have been extensively explored in recent years, as they are expected to perform better than large pieces of Si in accommodating extreme volume changes. Among these nanostructures, SiNWs with a crystalline core and an amorphous shell are especially interesting. Ideally, the crystalline Si core can serve as a mechanical support and efficient electrical conducting pathway, while the amorphous Si shell can store $Li^+$ ions.[16,18] If both parts are sustainable, the core–shell SiNWs are excellent for operation of Li-batteries with high cycle stability. Experimentally, the core–shell SiNWs were found to have high charge storage capacity and 90% capacity retention over 100 cycles.[16] Scanning electron microscopy (SEM) and transmission electron microscopy (TEM) studies show that the crystalline nanostructure of SiNWs can be retained after prolonged charging.[6,21–23]

To understand the high resistance of the crystalline Si core against Li penetration, several theoretical studies have been conducted, typically using the H-passivated SiNWs as models.[24–28] Results showed that Li atoms prefer to rapidly enter SiNWs, regardless of their size, which means that the Si core should have a very short lifetime under lithiation conditions, contradicting experimental observations. This strongly suggests that H-passivated SiNWs are inappropriate to represent actual boundary conditions in practical Li batteries, even though they are suitable for studies of other important issues such as the quantum confinement effect on band gap and impurity doping. While most Si atoms in H–SiNW models have a tetrahedral local symmetry and remain semiconducting, it is known that Li–Si mixtures around the crystalline Si core are amorphous and should have different electronic properties. Therefore, large-scale theoretical simulations using an actual core–shell model are necessary to investigate the segregation kinetics of Li insertion to better mimic the experimental environments.

## Calculation methods

Our calculations are performed using the Vienna *ab initio* simulation package (VASP)[29] in the framework of density functional theory (DFT). We use [001]-SiNWs with a diameter of 2.7 nm to build our models. About 15 Å wall-to-wall vacuum space is used in the lateral plane to reduce the interaction

[a]*Key Laboratory of Computational Physical Sciences (MOE), State Key Laboratory of Surface Physics, and Department of Physics, Fudan University, Shanghai 200433, China. E-mail: gxgrq1@gmail.com*

[b]*Department of Physics and Astronomy, University of California, Irvine, California 92697, USA*



This journal is © The Royal Society of Chemistry 2013

Published on 17 September 2013. Downloaded by Fudan University on 24/03/2014 03:37:17.

between the SiNWs and their images. The periodicity along the axis is set to 5.4307 Å, the lattice constant of bulk Si. We use the projector augmented wave (PAW) pseudopotential method[30] to describe the core–valence interactions, and the generalized gradient approximation (GGA)[31] for the exchange–correlation effect. The energy cutoff for the plane wave expansion is 400 eV; a $1 \times 1 \times 9$ $k$-point mesh is used to sample the essentially one-dimensional Brillouin zone. The AIMD simulations are performed in a canonical (NVT) ensemble with the Nosé–Hoover thermostat.[32] For the studies of electronic properties, all atomic positions at the end of AIMD simulations are further optimized according to the guidance of atomic forces, with a criterion that requires the calculated force on each atom smaller than 0.01 eV $Å^{-1}$.

In this paper, we report results of *ab initio* molecular dynamics (AIMD) simulations for Li segregation in [001]-SiNWs under ambient conditions. We found that Li atoms around the crystalline SiNWs may penetrate into them within one picosecond (ps) and form metallic amorphous Li–Si alloy shells. Interestingly, the insertion process self-stops when the crystalline Si core becomes sufficiently small, supporting the observation of Cui *et al.*[16] This unusual self-stopping of penetration results from attraction between the Li atoms and the metallized amorphous Li–Si shell. In contrast, Li is dragged toward the center of the H-passivated SiNWs by an electric force between the $Li^+$ ion and its 2s electron that is donated to the conduction state of SiNWs.

## Results and discussion

We first simulate the Li insertion process into SiNWs through AIMD simulations with a model that contains 47 Li atoms over the [001]-SiNWs as depicted in the left inset in Fig. 1a. To accelerate the Li segregation, our AIMD simulations are performed at 1100 K, with a time step of 2 fs. We monitor the evolvement of distribution patterns of Li atoms and total energies, and find that 7500–10 000 MD steps (or equivalently 15–20 ps) are adequate for Li atoms to settle down in SiNWs. Fig. 1a shows the evolution of free energies during AIMD simulations. It is obvious that the free energies only fluctuate in a small range after about 1 ps. This indicates that Li–SiNWs may reach their dynamical equilibrium very rapidly. The right inset in Fig. 1a shows a snapshot of the system at the end of AIMD simulations. One can see a characteristic structure of Li–SiNWs: a crystalline Si core and an amorphous Li–Si shell outside. We want to point out that the typical Li–Li distance is 3.0 Å in the amorphous region, so we believe that the periodicity of 5.4307 Å along the wire axis is sufficient to capture the essence of the local chemical environment for Li motion. As further support, we calculated a system with two Li atoms in bulk Si and found that the interaction energy between two Li atoms at a distance of 5.4307 Å apart is only about 0.05 eV (compared to the energy for the case with Li atoms 10 Å apart).

To better appreciate the evolution of Li distribution with respect to time, we plot the averaged distribution of Li, $n_{Li}$ $(r)$, in Fig. 1b, along with the most probable position of Li atoms as a function of time, $r_{Li}$ $(t)$, in the inset at different stages. It is

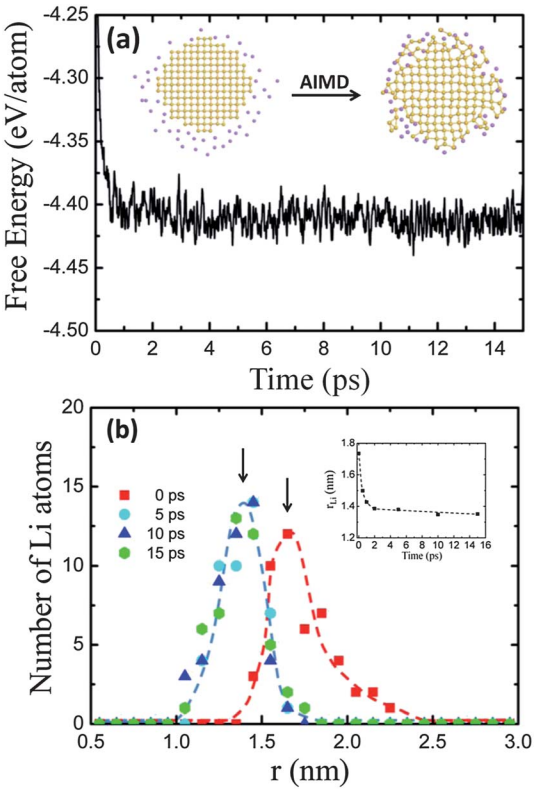


**Fig. 1** (a) The evolution of free energy during AIMD simulation for the Li-surrounded [001] SiNWs. The insets are the cross-sections of the SiNWs before and after the AIMD simulation, and Si and Li atoms are represented by yellow and violet balls, respectively. (b) The averaged radial distribution of Li atoms at $t = 0$, 5, 10 and 15 ps for the Li–SiNWs. The inset is the evolution of the most probable position of Li atoms.

obvious from Fig. 1a that Li atoms tend to quickly penetrate into the SiNWs and form an amorphous Li–Si shell, as also observed in experiments.[16] The $r_{Li}$ $(t)$ curve in the inset indicates that the inward segregation of Li basically stops within one ps. Furthermore, the $n_{Li}$ $(r)$ curves for $t = 5$ ps, 10 ps and 15 ps almost overlap with each other in Fig. 1b. Therefore, Li atoms essentially stop moving further into SiNWs once the radius of the crystalline core is reduced to about 1.0 nm.

To investigate whether this phenomenon depends on the number of Li atoms, we also perform AIMD simulations with 91 and 126 Li atoms on the same SiNWs. Fig. 2 shows the results of $n_{Li}$ $(r)$ at $t = 15$ ps for Li in SiNWs with three different concentrations. Strikingly, the remaining cores have nearly the same size, with a deviation less than 0.2 nm. Therefore, we can conclude that the size of the core in Li–SiNWs is almost independent of the concentration of Li. We want to emphasize that the temperature in our simulations is very high and the fact that the Si core still resists Li insertion for more than 15 ps is very important. This suggests that residual crystalline Si cores may remain in SiNW anodes even after prolonged charging.[6,21–23] Our AIMD simulations confirm the observation that SiNWs may retain a strong core region to withstand Li cycling, even though the size of the remaining cores may somewhat depend on the electrochemical potential in different experiments.[16]

Published on 17 September 2013. Downloaded by Fudan University on 24/03/2014 03:37:17.

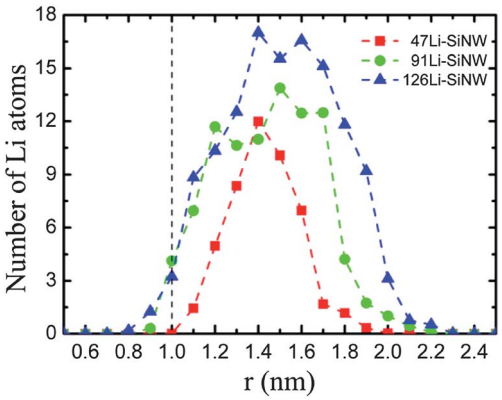


**Fig. 2** The averaged radial distribution of Li atoms at $t = 15$ ps for the SiNWs surrounded by 47, 91 and 126 Li atoms, respectively. The Li atoms stop with a Si core.

The core–shell boundaries can propagate through two processes: direct segregation of Li through interstitial channels and gradual amorphization through local Li–Si exchange. To explore the mechanism of the high resistivity of small Si cores against Li penetration, we first drag a single Li atom from the inner surface of the amorphous Li–Si shell and place it at different tetrahedral (Td) sites[24,25] in the Si core, as highlighted by the red and blue spots in the inset in Fig. 3a. The 47Li–SiNW model is used and we relax the atomic structure at each step. Using the case with Li at the central Td site as the reference, we find that the total energy increases monotonically as the Li atom moves from the shell into the core (Fig. 3a). Although the energy curves along two segregation paths differ slightly due to the low symmetry of the core–shell Li–SiNWs, it is clear that Li segregation through the interstitial channel into the small core region is energetically unfavorable. In fact, the steep increase of total energy indicates that the amorphous Li–Si shell is strongly attractive toward Li, which effectively pins the core–shell boundary and protects the crystalline shell from pulverization, in line with the AIMD results discussed above.

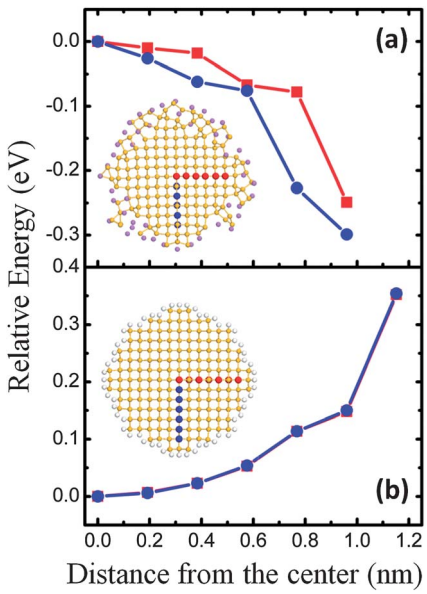


**Fig. 3** The relative energies when placing a Li atom at different Td sites along two directions as shown by the red and blue balls in the insets for the (a) Li–SiNWs and (b) H-passivated SiNWs. The energy when the Li atom is placed at the center site is taken as a reference.

Interestingly, the unusual self-stopping behavior of Li diffusion was not observed in previous studies that used the H-passivated SiNWs as templates,[24,25] as shown in the inset of Fig. 3b. When we move a Li atom along the Td sites from the surface to the center region of SiNWs, the total energy decreases monotonically as shown in Fig. 3b. The calculated energy barrier for Li hopping between adjacent Td sites in Si is about 0.5 eV, similar to the data in the literature.[24] Therefore, Li atoms may move straight to the center of the H–SiNWs under ambient conditions, so the crystalline phase in the entire wire can be damaged from inside. As a result, H–SiNWs pulverize under typical lithiation conditions, and hence cannot represent actual SiNWs in the experimental environment.

From the difference between H–SiNWs and Li–SiNWs, there is no doubt that boundary conditions are crucial for Li segregation. In the literature, the preference of Li atoms moving from the surface to central Td sites of the H–SiNWs was attributed to the quantum confinement effect and the surface strain effect.[24,25,33] However, we believe that it can be simply explained in terms of charge donation and electrostatic interaction. The curves of local density of states (LDOS) in Fig. 4a suggest that all Si atoms in H–SiNWs are semiconducting, with a band gap of about 1 eV. The Li atom donates its 2s electron to the lowest unoccupied molecular orbital (LUMO, or equivalently the conduction state) of the H–SiNWs and becomes a $Li^+$ ion. As displayed in Fig. 4b, the charge density near the conduction bands is rather delocalized in the cross-section of the wire and hence the 2s electron of Li spreads over the entire space in SiNWs. Using a model with homogeneous negative charge in a cylinder, it is very easy to find that the $Li^+$ ion experiences an attractive force toward the center of the wire and the magnitude of the force scales linearly with the radial position of the ion. The energy is hence a quadratic function of the distance of Li away from the center, the same trend as the calculated data shown in Fig. 3b. Therefore, the inward diffusion of Li into the semiconducting H–SiNWs is driven by the attraction between $Li^+$ ion and its 2s electron that is donated to the LUMO.

In contrast, the amorphous Li–Si shell in Li–SiNWs strongly prevents Li atoms from further segregation into SiNWs. The curve of total density of states (TDOS) in Fig. 5a suggests that Li–SiNWs are metallic, whereas the LDOS curves in Fig. 5b indicate that inner Si atoms are still semiconducting even though the energy gaps of Si atoms near the amorphous region are rather small. The charge distribution of states within $\pm 0.1$ eV is displayed in Fig. 5c. It is clear that these states are predominantly localized in the shell. Therefore, Si atoms within or near the shell are qualitatively different from those in the inner region or in H–SiNWs. The interaction between Li and metallized Si atoms is through orbital hybridization, which is much stronger than that through charge donation to the semiconducting Si atoms.


This journal is © The Royal Society of Chemistry 2013

Published on 17 September 2013. Downloaded by Fudan University on 24/03/2014 03:37:17.

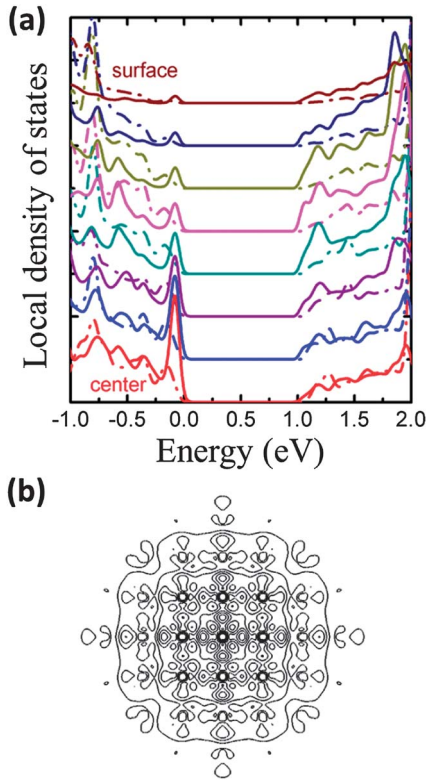


**Fig. 4** (a) Local density of states of different Si atoms from the center to the surface for the H-passivated SiNWs. The solid lines represent the situation when a Li atom is placed at the diffusion pathway. The dashed lines represent the situation without the placed Li atom. For these two situations, the Fermi energies are aligned. (b) The charge density of the orbitals near the conduction bands within the energy interval of 0.2 eV for the H-passivated SiNWs.

Through the discussion above, we can say that the active Li–Si shell effectively prohibits the straight penetration of Li into Li–SiNWs, and the core–shell boundary moves through the step-forward amorphization process. Now the question is why the core is vulnerable until its size is reduced to the nanometer scale. The exchange of Li and Si atoms and the subsequent formation of local Li–Si amorphous structures are accompanied by large local volume expansion and local stress. At the beginning of the lithiation process, this stress can be absorbed by sideway and outward relaxations. As the radius of the crystalline core shrinks, the stress in the shell develops a large inward pressure on the core across the curved interface.[34,35] Since this pressure is proportional to the inverse of the radius of the core, it eventually becomes sufficiently large to frustrate the amorphization process. With this picture in mind, one may expand the size of the crystalline core by applying a higher external pressure, *e.g.*, with carbon-coating in the experiment.[17,36] In addition, the stability of SiNWs can also be improved by implementing active elements in the Li–Si shell to attract Li atoms. Experimental attempts along this direction are desired.

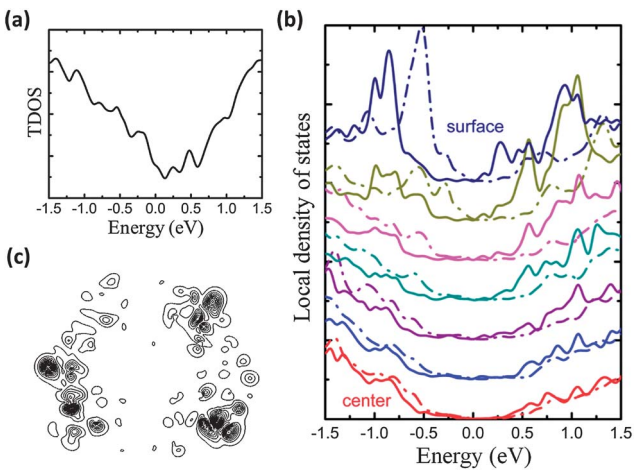


**Fig. 5** (a) Total density of states of the Li–SiNW system. (b) Local density of states of different Si atoms from the center to the surface for the Li–SiNWs. The solid lines represent the situation when a Li atom is placed at the diffusion pathway. The dashed lines represent the situation without the placed Li atom. (c) Partial charge density of the Li–SiNWs shown by contour lines. The partial density is integrated from the orbitals with energies from $E_F - 0.1$ eV to $E_F + 0.1$ eV, where $E_F$ is the Fermi energy.

## Conclusions

In summary, we performed *ab initio* molecular dynamics simulations within the framework of density functional theory to understand the segregation and amorphization processes of Li atoms into SiNWs. Although Li atoms can quickly penetrate into SiNWs at the onset, they essentially stop after a Li–Si amorphous shell is formed so that a small core region can be protected. The sustainability of a crystalline Si core in AIMD simulations at high temperature, 1100 K, and high Li concentration, up to 126 Li atoms in a cell, explains experimental observations. Further calculations for diffusion of a single Li atom revealed that this unusual self-stopping behavior results from the attractive force on Li from the metallized shell. We also explained the wrong trend predicted for Li segregation in semiconducting H–SiNWs.

## Acknowledgements

This work is partially supported by the Special Funds for Major State Basic Research, National Science Foundation of China, Ministry of Education and Shanghai Municipality. The calculations were performed in the Supercomputer Center of Fudan University. Work at UC Irvine was supported by DOE-BES (Grant no: DE-FG02-05ER46237) and by NERSC for computing time.

## References

1 Y. Cui, Q. Wei, H. Park and C. M. Lieber, *Science*, 2001, **293**, 1289.
2 Y. Cui and C. M. Lieber, *Science*, 2001, **291**, 851.
3 Y. Cui, Z. Zhong, D. Wang, W. U. Wang and C. M. Lieber, *Nano Lett.*, 2003, **3**, 149.
4 B. Tian, X. Zheng, T. J. Kempa, Y. Fang, N. Yu, G. Yu, J. Huang and C. M. Lieber, *Nature*, 2007, **449**, 885.
5 X. Wang, K. Q. Peng, X. J. Pan, X. Chen, Y. Yang, L. Li, X. M. Meng, W. J. Zhang and S. T. Lee, *Angew. Chem., Int. Ed.*, 2011, **50**, 9861.

Published on 17 September 2013. Downloaded by Fudan University on 24/03/2014 03:37:17.

6 C. K. Chan, H. Peng, G. Liu, K. Mcilwrath, X. F. Zhang, R. A. Huggins and Y. Cui, *Nat. Nanotechnol.*, 2008, **3**, 31.
7 B. A. Boukamp, G. C. Lesh and R. A. Huggins, *J. Electrochem. Soc.*, 1981, **128**, 725.
8 P. Johari, Y. Qi and V. B. Shenoy, *Nano Lett.*, 2011, **11**, 5494.
9 M. Gu, Z. Wang, J. G. Connell, D. E. Perea, L. J. Lauhon, F. Gao and C. Wang, *ACS Nano*, 2013, **7**, 6303.
10 K. Zhao, G. A. Tritsaris, M. Pharr, W. L. Wang, O. Okeke, Z. Suo, J. J. Vlassak and E. Kaxiras, *Nano Lett.*, 2012, **12**, 4397.
11 H. Yang, S. Huang, X. Huang, F. Fan, W. Liang, X. H. Liu, L. Q. Chen, J. Y. Huang, J. Li, T. Zhu and S. Zhang, *Nano Lett.*, 2012, **12**, 1953.
12 K. Zhao, W. L. Wang, J. Gregoire, M. Pharr, Z. Suo, J. J. Vlassak and E. Kaxiras, *Nano Lett.*, 2011, **11**, 2962.
13 E. D. Cubuk, W. L. Wang, K. Zhao, J. J. Vlassak, Z. Suo and E. Kaxiras, *Nano Lett.*, 2013, **13**, 2011.
14 S. H. Ng, J. Wang, D. Wexler, K. Konstantinov, Z. P. Guo and H. K. Liu, *Angew. Chem., Int. Ed.*, 2006, **45**, 6896.
15 H. Kim, B. Han, J. Choo and J. Cho, *Angew. Chem.*, 2008, **120**, 10305.
16 L. F. Cui, R. Ruffo, C. K. Chan, H. Peng and Y. Cui, *Nano Lett.*, 2009, **9**, 491.
17 C. K. Chan, R. N. Patel, M. J. O'Connell, B. A. Korgel and Y. Cui, *ACS Nano*, 2010, **4**, 1443.
18 H. Chen, J. Xu, P. C. Chen, X. Fang, J. Qiu, Y. Fu and C. Zhou, *ACS Nano*, 2011, **5**, 8383.
19 M. H. Park, M. G. Kim, J. Joo, K. Kim, J. Kim, S. Ahn, Y. Cui and J. Cho, *Nano Lett.*, 2009, **9**, 3844.
20 T. Song, J. Xia, J. H. Lee, D. H. Lee, M. S. Kwon, J. M. Choi, J. Wu, S. K. Doo, H. Chang, W. I. Park, D. S. Zang, H. Kim, Y. Huang, K. C. Hwang, J. A. Rogers and U. Paik, *Nano Lett.*, 2010, **10**, 1710.
21 N. Liu, L. Hu, M. T. McDowell, A. Jackson and Y. Cui, *ACS Nano*, 2011, **5**, 6487.
22 X. H. Liu, L. Q. Zhang, L. Zhong, Y. Liu, H. Zheng, J. W. Wang, J. H. Cho, S. A. Dayeh, S. T. Picraux, J. P. Sullivan, S. X. Mao, Z. Z. Ye and J. Y. Huang, *Nano Lett.*, 2011, **11**, 2251.
23 N. S. Choi, Y. Yao, Y. Cui and J. Cho, *J. Mater. Chem.*, 2011, **21**, 9825.
24 T. L. Chan and J. R. Chelikowsky, *Nano Lett.*, 2010, **10**, 821.
25 Q. Zhang, W. Zhang, W. Wan, Y. Cui and E. Wang, *Nano Lett.*, 2010, **10**, 3243.
26 Q. Zhang, Y. Cui and E. Wang, *J. Phys. Chem. C*, 2011, **115**, 9376.
27 R. Rurali, *Rev. Mod. Phys.*, 2010, **82**, 427.
28 J. R. Chelikowsky, M. M. G. Alemany, T. L. Chan and G. M. Dalpian, *Rep. Prog. Phys.*, 2011, **74**, 046501.
29 G. Kresse and J. Furthmuller, *Comput. Mater. Sci.*, 1996, **6**, 15.
30 P. E. Blochl, *Phys. Rev. B: Condens. Matter Mater. Phys.*, 1994, **50**, 17953.
31 J. P. Perdew, J. A. Chevary, S. H. Vosko, K. A. Jackson, M. R. Pederson, D. J. Singh and C. Fiolhais, *Phys. Rev. B: Condens. Matter Mater. Phys.*, 1992, **46**, 6671.
32 S. Nosé, *J. Chem. Phys.*, 1984, **81**, 511.
33 T. L. Chan, H. Kwak, J. H. Eom, S. B. Zhang and J. R. Chelikowsky, *Phys. Rev. B: Condens. Matter Mater. Phys.*, 2010, **82**, 115421.
34 K. Zhao, M. Pharr, Q. Wan, W. L. Wang, E. Kaxiras, J. J. Vlassak and Z. Suo, *J. Electrochem. Soc.*, 2012, **159**, A238.
35 M. T. McDowell, III, I. Ryu, S. W. Lee, C. Wang, W. D. Nix and Y. Cui, *Adv. Mater.*, 2012, **24**, 6034.
36 H. Chen, Z. Dong, Y. Fu and Y. Yang, *J. Solid State Electrochem.*, 2010, **14**, 1829.

 This journal is © The Royal Society of Chemistry 2013